



## Review

# Zooming in on disordered systems: Neutron reflection studies of proteins associated with fluid membranes<sup>☆</sup>



Frank Heinrich, Mathias Lösche<sup>\*</sup>

Physics Department, Carnegie Mellon University, Pittsburgh, PA, U.S.A.  
NIST Center for Neutron Research, Gaithersburg, MD, U.S.A.

## ARTICLE INFO

## Article history:

Received 24 December 2013  
Received in revised form 13 March 2014  
Accepted 17 March 2014  
Available online 25 March 2014

## Keywords:

Membrane structure  
Membrane protein  
Scattering techniques  
Composition-space modeling  
MD simulation

## ABSTRACT

Neutron reflectometry (NR) is an emerging experimental technique for the structural characterization of proteins interacting with fluid bilayer membranes under conditions that mimic closely the cellular environment. Thus, cellular processes can be emulated in artificial systems and their molecular basis studied by adding cellular components one at a time in a well-controlled environment while the resulting structures, or structural changes in response to external cues, are monitored with neutron reflection. In recent years, sample environments, data collection strategies and data analysis were continuously refined. The combination of these improvements increases the information which can be obtained from NR to an extent that enables structural characterization of protein-membrane complexes at a length scale that exceeds the resolution of the measurement by far. Ultimately, the combination of NR with molecular dynamics (MD) simulations can be used to cross-validate the results of the two techniques and provide atomic-scale structural models. This review discusses these developments in detail and demonstrates how they provide new windows into relevant biomedical problems. This article is part of a Special Issue entitled: Interfacially Active Peptides and Proteins. Guest Editors: William C. Wimley and Kalina Hristova.

© 2014 Elsevier B.V. All rights reserved.

## Contents

1.	Introduction . . . . .	2342
2.	Methods . . . . .	2342
2.1.	Artificial lipid bilayer membranes . . . . .	2342
2.2.	Neutron reflectometry . . . . .	2343
2.3.	Modeling of membrane-associated proteins . . . . .	2344
2.3.1.	The continuous distribution model . . . . .	2344
2.3.2.	Uncertainty analysis as a basis for advanced modeling . . . . .	2344
2.3.3.	Modeling the envelopes of membrane-associated proteins . . . . .	2344
2.3.4.	Using structural data . . . . .	2344
2.4.	Model-independent spline methods . . . . .	2345
2.5.	Combining protein envelopes with the lipid membrane model . . . . .	2345
3.	Protein association with lipid membranes: Recent accomplishments . . . . .	2345
3.1.	Rigid body modeling . . . . .	2345
3.2.	Protein localization on membranes . . . . .	2346
3.3.	Determination of orientation and localization . . . . .	2346
3.4.	Proteins with intrinsic disorder . . . . .	2346
3.5.	Complementing NR with MD simulations . . . . .	2346
3.6.	Triggered conformational changes . . . . .	2347
4.	Conclusions . . . . .	2347
	Acknowledgments . . . . .	2348
	References . . . . .	2348

<sup>☆</sup> This article is part of a Special Issue entitled: Interfacially Active Peptides and Proteins. Guest Editors: William C. Wimley and Kalina Hristova.

<sup>\*</sup> Corresponding author at: Physics Dept., Carnegie Mellon University, 5000 Forbes Ave., Pittsburgh, PA 15213-3890, U.S.A.

E-mail address: [quenched@cmu.edu](mailto:quenched@cmu.edu) (M. Lösche).

## 1. Introduction

Transmembrane and membrane-associated proteins play crucial roles in a broad range of cellular processes [1]. At least 30% of mammalian genes encode membrane proteins. Their roles in cells are indispensable, for example as mediators of cell signaling [2–4], information transduction and processing [5], as well as in cellular morphogenesis. Membrane proteins control selectivity of energy, material and information transfer into and out of the cell and between intracellular compartments, as well as vesicular transport within the cell [1]. Consequently, anomalies often result in disease states, ranging from cancer and premature senescence to neurological disorders [3]. In addition, since membranes provide the natural barrier between the cell and its environment, toxin and pathogen entry into cells inevitably involve protein–membrane interactions [6]. Yet, established techniques to determine molecular details of the association of proteins with lipid bilayers – the matrix they associate with – lag better-developed methods of structural biology such as protein crystallography and NMR spectroscopy dramatically. The leading reason is that proteins embedded or adsorbed to functionally intact, in-plane fluid lipid bilayers are notoriously difficult to study, as the classical crystal-based or solution-based characterization techniques are inadequate. As a result, our knowledge of high-resolution structures of membrane proteins in their natural membrane environment, and consequently also of mechanisms of their action and cellular control, is critically underdeveloped.

For more than 25 years, membrane protein structures have been determined by X-ray diffraction from crystals grown from detergent-solubilized protein solutions [7,8]. This technique provides atomic-scale 3D structures. However, it shows detergent molecules at those protein surfaces natively embedded in the membrane. While the art of crystal growth remains tedious, this technique still provides the bulk of the more than 400 unique high-resolution structures of transmembrane proteins known to date [9]. While membrane-peripheral proteins are usually not amenable to crystallization in detergent, many such membrane proteins are buffer soluble, because they shuttle between the cytosol and membrane surfaces within the cell, and can therefore be directly crystallized from detergent-free solutions. In both cases, protein–membrane association can only be estimated (transmembrane proteins) or is not known at all. In comparison to X-ray crystallography, electron diffraction from two-dimensional (2D) lipid/protein co-crystals [10,11], protein crystallization in cubic lipid phases [12] and solid-state NMR [13] or NMR on proteins solubilized in nanodiscs [14] have only played minor roles in the determination of high-resolution internal membrane protein structures so far. However, all these methods yield crucial information when it comes to determine the structure of protein/membrane complexes using scattering techniques.

X-ray and neutron scattering techniques, in distinction from crystal diffraction, provide capabilities to characterize disordered systems but lack the intrinsic resolution to study protein–membrane complexes on length scales shorter than nanometers. Nevertheless, in connection with complementing information from other sources they provide a novel window into high-resolution structures. In particular, neutron reflectometry as a surface-sensitive scattering technique has the potential to characterize protein–membrane complexes with unprecedented resolution, following the development of carefully engineered sample formats and dedicated data evaluation and modeling techniques. Indeed, recent progress in this area has been encouraging. Measuring the neutron reflection (NR) from engineered planar membrane mimics which retain their in-plane lipid fluidity [15], we showed that the out-of-plane localization of transmembrane proteins with known internal structures can be achieved with Ångström precision [16]. Extending work by Schlossman and collaborators using X-ray reflectometry [17, 18], it was recently demonstrated that both the penetration depth into the lipid membrane and orientation on the bilayer can be determined for membrane-associated peripheral proteins with high precision using NR [19–21]. Using molecular dynamics (MD) simulations to

interpret NR results we showed that the PTEN tumor suppressor, a lipid phosphatase whose structure was partially determined with X-ray crystallography [22], has slightly different atomic-scale structures in the crystal, in solution and in its membrane-bound state [23]. Finally, since NR characterizes protein structures on single bilayers, this technique is capable to determine structural changes that follow external cues *in situ*. This was demonstrated by the recent discovery that membrane-bound full-length gag from HIV-1 undergoes a dramatic structural reorganization upon nucleic acid binding [24]. Similarly, extensive studies of the conformation of HIV-1 Nef determined the impact of the composition and structure of the lipid membrane on protein organization [25,26]. In this review we describe recent accomplishments and discuss the technological developments that lay the basis for these advances.

## 2. Methods

### 2.1. Artificial lipid bilayer membranes

Current structural studies of lipid bilayer membranes and associated proteins with NR require the preparation of the biological interface on solid supports that are flat and atomically smooth over a large area (tens of square centimeters) [27]. This excludes investigations of natural membranes *in vivo* but can be readily achieved with artificial membrane systems. Types of artificial, supported membrane systems relevant for NR are solid-supported membranes [28], hybrid membranes [29–33], tethered membranes [34,35], polymer-cushioned membranes [36–39], and floating membranes [40,41]. Comprehensive reviews on supported lipid bilayer membranes can be found in the literature [42–45]. Langmuir monolayers of lipids at the air–water interface constitute a separate class of model systems [46].

A versatile lipid model system, optimized to meet several crucial requirements for high-resolution NR studies, is the sparsely tethered lipid bilayer membrane (stBLM, see Fig. 1). Grafted onto a planar solid support (typically a Si wafer or glass slide) that is terminated with a 10 nm to 200 nm thick gold film, stBLMs are excellent mimics of natural membranes with respect to lipid fluidity and structure [15]. They can be prepared using a large variety of lipids, including zwitterionic (phosphatidylcholine or phosphatidylethanolamine) or anionic lipids (phosphatidylserine, phosphatidylglycerol, phosphatidylinositol, or phosphatidic acid) with saturated or unsaturated chains, sterols, and functional components such as phosphatidylinositol phosphate lipids. Spacing of the synthetic tether lipids, grafted to the terminal gold film of the substrate through thiol chemistry and (typically) an oligo(ethyleneoxide) linker [47–49] (Fig. 1), is achieved by co-adsorption with  $\beta$ -mercaptoethanol ( $\beta$ ME). stBLMs can be prepared virtually defect-free [50], which prohibits unspecific protein adsorption to exposed support areas that would interfere with structural characterization of the membrane-associated protein. Of similar importance, stBLMs are stable for the time scale of NR experiments which can be on the order of days with current technology [51]. The lipid membrane in an stBLM is separated from the solid support which otherwise might interact with incorporated proteins [47]. stBLMs exhibit low interfacial roughness, because of their proximity to the substrate ( $\approx 20$  Å). From a scattering point of view, this is important for achieving high resolution of the underlying structures [27]. On the other hand, the proximity of the substrate to the membrane and interference with the tethering chemistry – typically a molar fraction of 50% of the lipids located in the inner lipid leaflet are tether lipids – may limit the reconstitution of membrane proteins with large extramembraneous domains.

A variety of surface-sensitive techniques can be applied to the stBLM platform, aiding the characterization of biological systems of interest. For example, the gold-coated solid support allows for surface plasmon resonance (SPR) spectroscopy [21] and electrical impedance spectroscopy (EIS) [47–50]. Yet, the gold films are so thin that the system remains amenable to characterization with fluorescence techniques, for

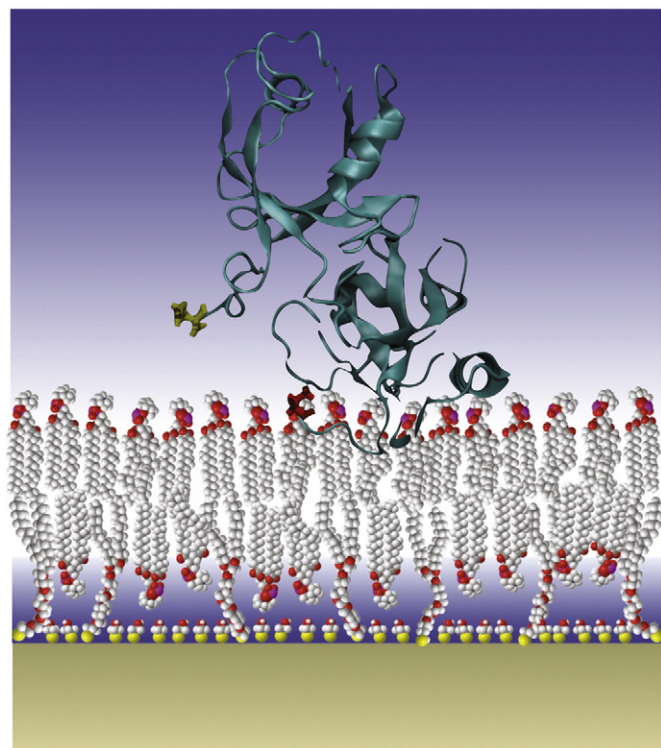


**Fig. 1.** Cartoon of a sparsely tethered bilayer lipid membrane (stBLM). Following the formation of a self-assembled monolayer of PEGylated lipidic tether molecules, grafted to a gold surface via thiol bonds, the bilayer is completed using either vesicle fusion or rapid solvent exchange. Sparse grafting of tethers is achieved by co-adsorption with  $\beta$ ME. This sketch also shows the structure of a membrane-associated protein, GRASP55, whose orientation and membrane penetration have been determined with neutron reflectometry [19].

example, imaging [52] or fluorescence correlation spectroscopy (FCS) [15]. The flat solid support allows for immersed atomic force microscopy (AFM) [53].

## 2.2. Neutron reflectometry

Neutron reflectometry (NR) for biological systems is an established technique [45,54,55], available at all major neutron scattering facilities world-wide [56,57]. While averaging over structural features in-plane, NR yields one-dimensional information in the perpendicular direction in the form of neutron scattering length density (nSLD) profiles from which molecular or sub-molecular component distributions (or component volume occupancy, CVO, profiles) of an interfacial architecture along the interface normal can be deduced. As demonstrated in Fig. 2, the NR is described by nSLD distributions (inset in Fig. 2A) that follow directly from the in-plane densities of molecular subcomponents (Fig. 2B) – for example, of the lipid headgroups in the surface of a bilayer membrane – as a function of distance  $z$  from a reference plane. In a sufficiently thin slice,  $dz$ , parallel to the membrane surface, the normalized area occupied by a particular component then provides its *volume occupancy* as a function of  $z$ .

Although the loss of phase information is a general problem in scattering that prevents direct data inversion, robust modeling strategies, developed for structures that are approximately known, circumvent this problem. Since NR probes the structural profile along the membrane normal, any in-plane information has to be inferred from a 1D profile. However, complementing information such as volumetric data, chemical connectivity, high-resolution structures or MD simulations aid greatly to fill that gap. Deuteration of specific molecular components is a powerful tool to localize these components in neutron

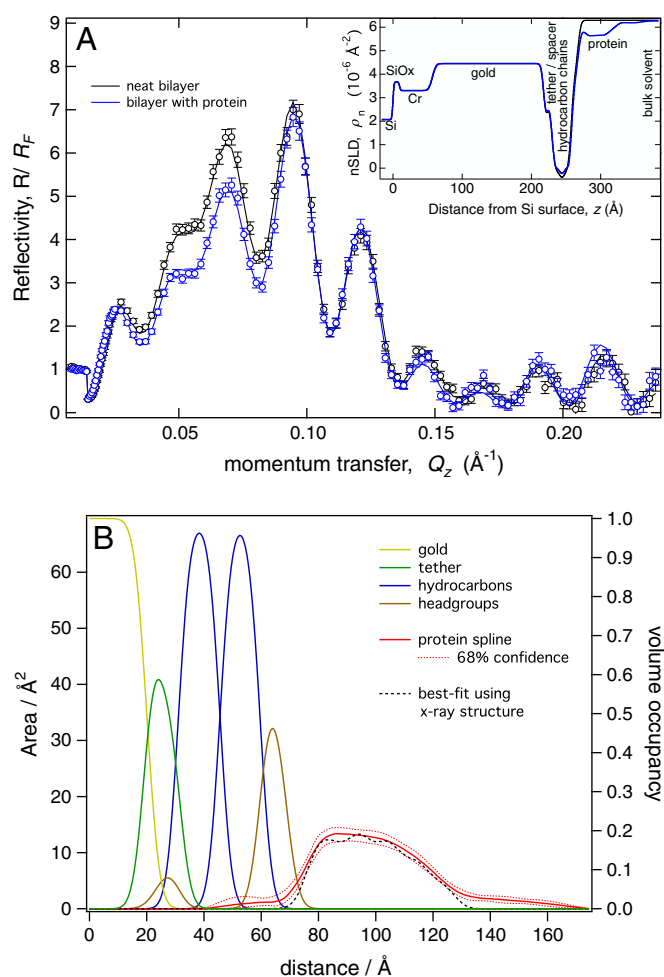


**Fig. 2.** (A) Typical NR spectra for an stBLM (9:1 DOPC:DOGS-NTA) before and after protein (GRASP55) association, measured using  $D_2O$ -based bulk solvent. The momentum transfer  $Q_z$  increases with the incident angle of the neutron beam. The reflectivity (i.e., the flux ratio of reflected and incident neutrons) is normalized to the Fresnel reflectivity  $R_F$  (i.e., the ideal reflectivity between the two bulk media, in this example silicon and  $D_2O$ -based bulk solvent). This presentation emphasizes the interference effects at the stratified gold/membrane structure. Inset: Modeled nSLD profiles along the membrane normal that describes the experimental data (lines in main panel). Changes in the nSLD profile due to the associated protein are readily visible. It is still common practice to model an nSLD profile as a sequence of layers, each with constant nSLD, and refine its structure given the data, then interpret the result in terms of the molecular composition. Here, we advocate a composition-space data refinement approach that models the chemical architecture in terms of its component volume occupancy (CVO) distributions directly, resulting in a real-space structure from which multiple isotopically varied nSLD profiles, and consequently the associated reflectivity spectra, are obtained. (B) Composition-space model of the GRASP55/membrane complex. The lipid bilayer is parameterized using the continuous distribution model [63]. For simplicity, certain sub-molecular components that were modeled separately have been combined in this representation. The six distinct distributions shown represent the outer 20 Å of the gold substrate layer, the hydrophilic region of the tether molecules and  $\beta$ ME that form the hydrated sub-membrane space, the substrate-proximal lipid headgroups and (lipid and tether) hydrocarbon chains, the substrate-distal lipid hydrocarbon chains and headgroups. The protein's cross-section as a function of distance from the solid substrate ("protein envelope") has been determined by fitting to a monotonic Hermite spline. Uncertainties were quantified by a Monte Carlo Markov Chain method and are displayed for the protein envelope as 68% confidence bands. Uncertainty intervals for the molecular distributions of the tethered bilayer and the substrate are omitted for clarity, and only best-fit distributions are displayed.

scattering and can be applied to resolve a specific constituent of a protein complex.

A typical NR experiment to characterize a membrane-associated protein on an stBLM (Fig. 2) uses a flow-through cell [33] that enables buffer exchange *in situ*. This allows to study a sample under different isotopic buffer compositions or to determine the response of the sample structure to external manipulations, such as the introduction of protein

or small molecules following characterization of the pristine bilayer, or the change of the salt concentration or of the pH of the buffer. Every condition is typically measured at least twice in isotopically distinct bulk solvents (contrasts), for example, in H<sub>2</sub>O- and D<sub>2</sub>O-based buffer solutions. This allows distinguishing between scattering contributions by the solvent and by other interfacial components. Co-refinement of these different sets of reflectivity data from one unique sample measured under a variety of conditions then allows determining CVO profiles with the high confidence [57]. It also permits the precise quantification of changes of the interfacial structure due to protein interaction with the membrane. A magnetic reference layer technique can be used to further increase the effective resolution of the neutron experiment, albeit currently at the cost of measurement time [58,59].

### 2.3. Modeling of membrane-associated proteins

#### 2.3.1. The continuous distribution model

In the past, (neutron or X-ray) reflectivity data analysis has been dominated by the slab model [60] which describes the interfacial structure in terms of stratified slabs of constant scattering length density. This “box” model was greatly successful because of its close relationship with the optical matrix method that allows for an efficient calculation of the parent reflectivity spectrum. However, the slab model is impractical when applied to complex molecular architectures that consist of spatially intermixing sub-molecular groups. The transition to structure-based composition-space modeling [61,62] allowed (a) to build detailed molecular models, (b) to directly parameterize relevant structural features of the bio-molecular film, and (c) to include external information about the chemical and physical properties of the molecular constituents in the modeling.

We recently developed a composition-space approach that uses error functions for modeling continuous distributions of molecular components within bio-molecular interfacial structures (Fig. 2 B) [63]. Its implementation for lipid bilayer membranes was validated against distributions of sub-molecular fragments obtained from MD simulations. This modeling strategy provides high flexibility to arrange molecular groups in space while physically valid boundary conditions are intrinsically maintained. For example, the continuous distribution model achieves volume filling of complex molecular architectures intrinsically, in distinction to composition-space models based on Gaussian distributions [61,64,65]. This feature makes the new parameterization particularly suited for complex molecular architectures such as the stBLM systems with incorporated or adsorbed proteins [16,20,21], and it can also be readily applied to lipid bilayers physisorbed on solid supports, self-assembled monolayers (SAMs) or Langmuir monolayers on air-water surfaces.

#### 2.3.2. Uncertainty analysis as a basis for advanced modeling

For a number of reasons, a rigorous method to determine parameter uncertainties is another prerequisite for the evaluation of NR data from bio-molecular architectures. First, such a method is essential to test any new model for over- and under-parameterization, thereby quantifying the information content of the data and helping the investigator to adjust the complexity of the model accordingly. In practical terms, this is an iterative process in which parameter space is expanded and reduced in a series of model fits with uncertainty analyses to determine the maximal number of parameters for which acceptable confidence intervals can be obtained. Such checks, however, do not validate the choice of the model itself. Second, model-independent parameterizations are often employed to describe components of the molecular architecture for which little prior knowledge, for example no information on the internal structure, exists. These, again, need to be quantified for their significance with a bias-free determination of their parameter uncertainties. Here, this is even the more critical as, by their very construction, such models contain a larger number of degrees of freedom. In general, any single set of nSLD or CVO profiles that describe the experimental

data sufficiently well may be meaningless unless combined with information about their uncertainty.

We routinely use Monte Carlo simulations [48] or, more recently, a Monte Carlo Markov Chain method [57] to determine uncertainties. Both are statistical methods that also quantify parameter correlations, thereby providing additional information that can be efficiently used for model optimization. They are superior to the Levenberg–Marquardt algorithm, which assumes a parabolic minimum of the fit cost function. Moreover, the Monte Carlo-based methods can be used to determine uncertainties of properties that depend on parameter combinations. For bilayer membranes, this includes the area per lipid molecule, a characteristic function of lipid structure that has been determined for different lipid species in various model membrane formats with high precision [65–67]. Last but not least, CVO distributions and basic nSLD profiles can be determined with their confidence bands (Fig. 2B), which is an informative way to represent uncertainties.

#### 2.3.3. Modeling the envelopes of membrane-associated proteins

The structural information revealed by NR about protein–membrane complexes is in the form of cross-sectional area profiles  $A(z)$  as a function of distance  $z$  from an interface. We refer to the CVO profile of proteins as “protein envelopes” (Fig. 2B). The modeling strategy for determining the envelope of a membrane-associated protein depends on the prior knowledge of its internal structure. If a (partial) high-resolution crystal or NMR structure is available, this information can be directly utilized in the data modeling, as shown below. On the other hand, for proteins of unknown structure and for disordered proteins, model-independent parameterizations provide a valuable tool for structure determination. For partially disordered proteins with known structures of the ordered domain(s), a comparison of the two approaches may help identify the organization of the disordered protein regions [21]. Finally, isotopic labeling of a particular protein or of specific regions in a protein can reveal the contribution of that protein (region) to the overall scattering in a complex of proteins associated with the bilayer membrane.

#### 2.3.4. Using structural data

High-resolution structural data for a protein as a source of prior information can be used within NR data analysis using rigid body modeling. A crystal structure provides the 3D distribution of nSLD within the protein and therefore its shape anisotropy, allowing to parameterize protein association with the membrane in terms of its penetration depth and orientation with respect to the interface. Importantly, this information is gleaned despite the fact that NR provides only 1D profiles along  $z$  while averaging over the  $x$ – $y$ -plane, due to rigorously coupling the 3D information from the crystal structure with the reflectivity data.

In technical terms, the protein structure is sliced into slabs of thickness  $dz$ . For each slab, the cross-sectional area  $A$  and the contained scattering length  $nSL$  are determined.  $dz$  is typically set to 0.5 Å. The nSL is calculated by adding up all the coherent cross sections [68] of atoms of the protein that fall within a certain slab.  $A$  can be determined by calculating the solvent accessible volume of the protein [69,70], and slicing it using the same sequence of slabs. An alternative method for calculating  $A$  makes use of experimentally determined average volumes per amino acid, for example from SANS contrast matching experiments [71]. To implement the determination of protein orientation, the protein is rotated and sliced in discrete steps of typically 5° in two of the three Euler angles, while the third Euler angle is irrelevant due to the rotational symmetry of the problem [17,20]. In the fit, the two significant Euler angles are continuously varied by computing intermediates between the discrete orientations using a tri-cubic local interpolation that ensures a continuous first derivative of the cost function [72]. The thus discretized protein model can be readily combined with the composition-space model of a tethered lipid bilayer.

## 2.4. Model-independent spline methods

If independent structural information is not available, model-independent parameterizations may be used to interpret NR data [20, 24,73–75]. A particularly intuitive choice is spline functions, such as the parametric cubic B-spline [76–79], because they allow for local real-space modeling of smooth nSLD or VCO profiles with a set of  $n$  control points  $\{(z_0; \rho_0), \dots, (z_n; \rho_n)\}$  or  $\{(z_0; A_0), \dots, (z_n; A_n)\}$ . The practical implementation of this particular spline, however, is rather difficult. Depending on the set of control points, the resulting profile may exhibit unphysical cusps and loops. Furthermore, the parametric cubic B-spline does not generally pass through the control points, which is a major obstacle for its practical application. We therefore chose simpler Hermite splines, implemented as Catmull-Rom [21,80] or, more recently, monotonic Hermite splines [19,81], which do not have those disadvantages and, for the monotonic Hermite spline, avoid overshooting in the vicinity of control points. While Hermite splines provide a smaller function space than parametric cubic B-splines, we empirically found the flexibility of the Hermite spline to be sufficient for the modeling of protein envelopes from current NR data. The flexibility of the Hermite splines is maximized by allowing the control points to deviate to some extent from their initially equally spaced center positions on  $z$ .

## 2.5. Combining protein envelopes with the lipid membrane model

Combination of the continuous distribution model of a lipid bilayer with a penetrating protein envelope is not straightforward. Because different proteins affect bilayer structures differently, there is no unique procedure that fits all situations. Protein molecules interact with membranes locally, and even if a particular protein binds the membrane strongly, it typically covers only 20% to 30% of the available surface, leaving the remaining membrane regions largely unaffected. Furthermore, simplifying assumptions, in particular about lipid reorganization, need to be made. In practical terms, the merging of the two contributions is

implemented by determining at each discrete location  $z$  if lipids are displaced from the bilayer, and removing material accordingly in the model. When replacing a certain fraction of lipid chains, the same fraction of headgroup material is removed from the system, or vice versa. While the bilayer model is typically adjusted in its hydrocarbon thickness and overall completeness to account for protein interactions, the shapes of the distributions of sub-molecular fragments are not altered. This procedure yields satisfactory modeling results, according to our experience. If the need arises to introduce a more exact modeling of lipid rearrangements, work by Politsch [82–86] on modeling of 2D intermolecular configurations might be a good starting point for further development.

## 3. Protein association with lipid membranes: Recent accomplishments

### 3.1. Rigid body modeling

For the purpose of NR data analysis, we classify a protein as being rigid, if it can be assumed that its high-resolution structure, for example from crystallography, remains relevant upon binding of the protein to the membrane. Neutron or X-ray data from membrane-associated rigid proteins can be analyzed using crystal or NMR structures to gain precise information about orientation and membrane penetration. For two-dimensional sheet crystals of proteins grown *in situ* underneath floating Langmuir monolayers of lipid, this has been early on demonstrated with neutron reflection [87] and X-ray reflection at synchrotron sources [46]. More recently, Schlossman et al. characterized the membrane association of the p40<sup>phox</sup>-PX domain [18] and the PKC $\alpha$ -C2 domain [17]. For bilayer-associated proteins, this had been demonstrated for the membrane interaction of the bacterial toxin,  $\alpha$ -hemolysin [16], and for the matrix domain of the HIV-1 viral envelope protein Gag [20].

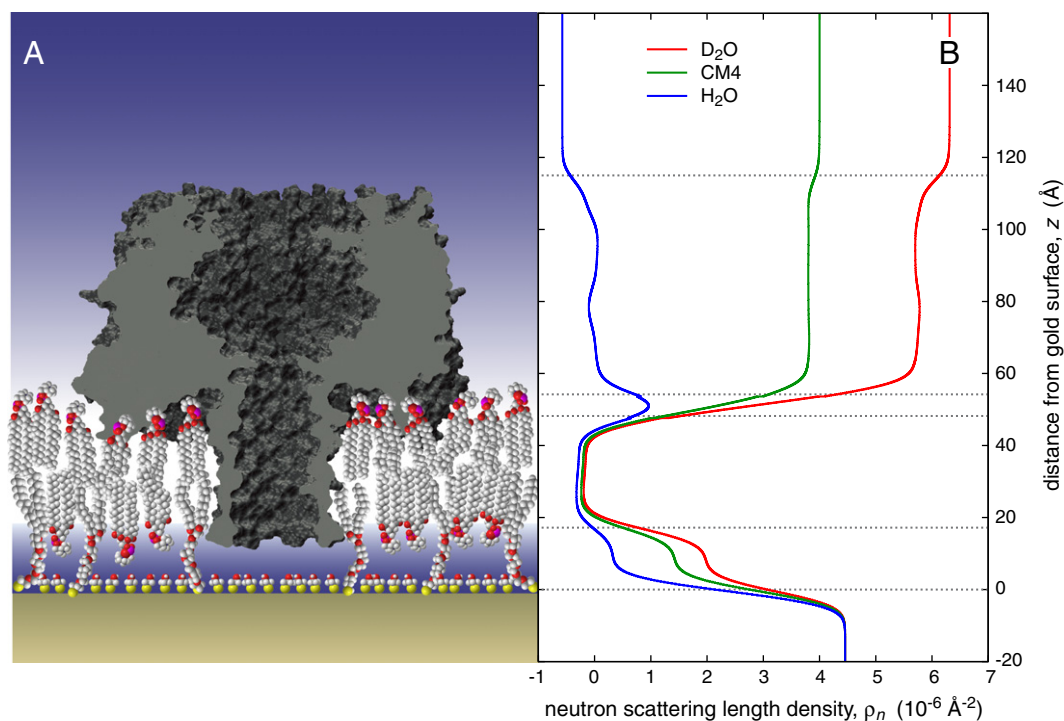


**Fig. 3.** (A) Molecular cartoon, drawn to scale, and (B) nSLD profile of  $\alpha$ -hemolysin reconstituted in an stBLM [16]. NR was measured in three solvent contrasts with buffers based on H<sub>2</sub>O, D<sub>2</sub>O and a 1:2 mixture (termed “CM4”). The data were analyzed using a traditional box model. The protein envelope was obtained from the X-ray structure via micro-slicing and was combined with the lipid bilayer in the model under variation of the penetration depth.

### 3.2. Protein localization on membranes

An early feasibility study showed that rigid transmembrane proteins, such as the membrane pore  $\alpha$ -hemolysin, can be localized within an artificial, fluid bilayer with a precision of  $\approx 1$  Å using NR (Fig. 3) [16]. In this work, an stBLM [47] was initially characterized as prepared before exposing it to dissolved  $\alpha$ -hemolysin monomers. The formation of functional heptameric membrane pores was independently confirmed by comparing the ion conductance and its blockage with dissolved poly(ethylene glycol) as a function of polymer size. From the quantitative correspondence of these conductivity screens of  $\alpha$ -hemolysin in stBLMs with  $\alpha$ -hemolysin reconstituted in free-standing bilayers [88], it was concluded that the protein indeed organized into its  $\beta$ -barrel structure. Thereby, the high-resolution X-ray structure [89] could be used for data modeling. Because of the protein symmetry, it was then sufficient to allow only the protein surface coverage and penetration depth to vary. The protein orientation was fixed with the symmetry axis of the pore remaining parallel to the membrane normal. Achieving a high lateral density of reconstituted protein,  $\approx 33\%$  of the closest hexagonal packing, the penetration depth of the protein could be determined within  $\pm 1$  Å within a 68% confidence limit. In the resulting membrane complex,  $\alpha$ -hemolysin brings hydrophilic residues which line the membrane-proximal region of its cap in close contact with the lipid bilayer. The stem penetrates the hydrocarbon core of the lipid bilayer in its entirety, protruding only marginally from the proximal headgroup region (Fig. 3).

### 3.3. Determination of orientation and localization

If a membrane protein with radial symmetry, such as  $\alpha$ -hemolysin, inserts into the membrane, there is little doubt that the symmetry axis is aligned with the bilayer normal. However, most proteins lack such symmetry, and therefore their penetration depth and orientation need to be simultaneously established. To determine protein orientation, two Euler angles (see Fig. 4) are fitted as additional continuous parameters in the data refinement. For every combination of Euler angles, the nSLD and CVO profiles are calculated from the high-resolution structure, and combined with the lipid bilayer profile to calculate the expected NR spectrum of each configuration. The results from these angular anchor points are then interpolated to obtain the spectra for a (quasi-) continuous distribution of Euler angles. This procedure was recently applied [20] to interpret the NR from stBLM-associated HIV-1 gag matrix (MA) domain [90]. Even with the simultaneous determination of penetration depth and protein orientation, the out-of-plane localization on the bilayer could be determined with a precision of  $\approx 3$  Å and the orientations within  $\approx 10^\circ$ . Because the distributions of functional subgroups of the lipid molecules are also resolved in these measurements, this allowed an analysis of the interactions of specific groups of amino acid residues with various parts of the lipid membrane.

### 3.4. Proteins with intrinsic disorder

NR data from proteins that contain disordered regions require analysis methods beyond rigid body modeling. Model-independent methods can be used to determine the molecular envelopes of proteins without prior structural information. A large class of problems to which those methods can be applied is the conformation of membrane-associated peptides [91]. With increasing frequency, Monte Carlo and MD simulation techniques are combined with model-independent methods to solve such structures with sparse prior information.

Oriented multi-bilayer membranes have been extensively used to determine the distribution of disordered lipid components across bilayers with 1D crystallography approaches [66,92–94]. However, this sample format does not allow for *in-situ* manipulations. In contrast, fluid-immersed single-bilayer stBLMs facilitate studies of the response of protein–membrane complex structures to external triggers. This

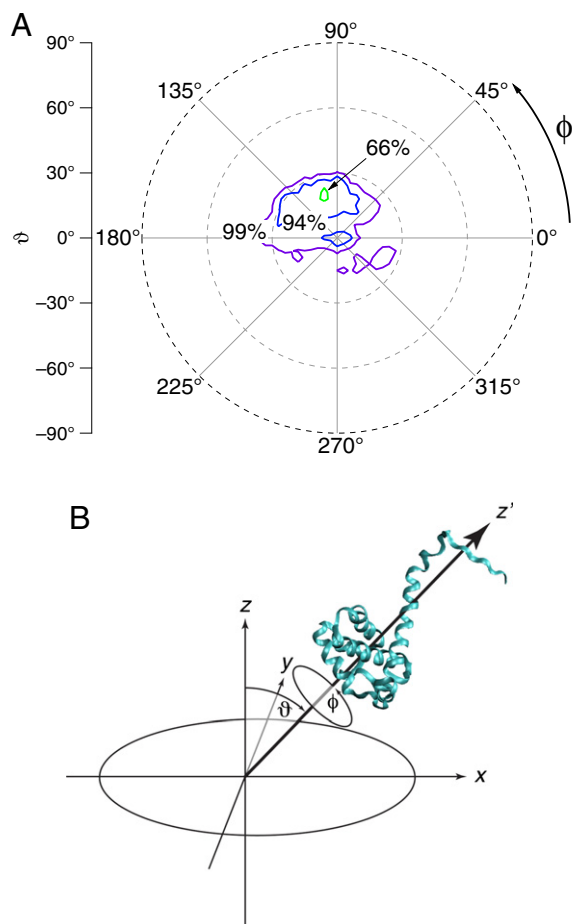


**Fig. 4.** Probability polar plot for orientations of HIV-1 matrix domain on the lipid membrane in an stBLM. 66%, 94%, and 99% confidence intervals are indicated. NR is sensitive to two Euler angles: the rotation  $\phi$  around the long principal axis  $z'$  of the protein, and the tilt  $\theta$  of this principal axis with respect to the membrane normal  $z$ .

opens opportunities to emulate basic cellular processes *in vitro* and sample their associated structural responses. Such a molecular trigger has been used, for example, to induce the extension of the membrane-bound HIV-1 Gag polyprotein, a string of protein domains ligated by flexible peptide connections. When the polyprotein in aqueous buffer is allowed to incubate an anionic membrane, a conformation was observed consistent with the model that both the MA and the terminal nucleocapsid (NC) domain bind to the bilayer surface, with the intermediary capsid (CA) domain disjoined from the membrane. Upon incubating the protein–membrane complex with short nucleic acid snippets that emulate RNA binding, the NC domain was released from the lipid surface, leading to an extended structure of the full-length gag. The observed extended structure is presumably required to enable lateral interactions between CA which may be critical for capsid formation [24]. Another exciting example for protein reorganization following an external cue is the conformational change of HIV-1 Nef at the lipid membrane [25,26], triggered by the insertion of its N-terminal myristate group.

### 3.5. Complementing NR with MD simulations

The most detailed NR study of a membrane-associated protein to date was accomplished by merging the partially known crystal structure of the tumor suppressor and signaling protein PTEN [22] with a large-scale, all-atom MD simulation to interpret NR results [21,23]. A 500 ns long MD simulation settled into a protein/membrane complex structure that was in agreement with the experimentally determined

protein envelope, revealing the conformation of PTEN's functionally important, disordered C-terminal tail which is not represented in the high-resolution structure of a truncated PTEN protein (Fig. 5). Differences between the X-ray structure of the protein, its solution structure and its membrane-associated structure were obtained from the MD simulations and showed subtle changes that the protein undergoes upon binding to the membrane. These differences *per se* were indistinguishable in the scattering data due to the limited resolution of the NR experiments.

Future NR data analysis is poised to connect more tightly with molecular simulations, beyond a mere comparison of experimental structural profiles with independently obtained simulation results. A promising approach is steered MD simulations, biased to capture the experimental results at intrinsically lower resolution. This strategy was successfully applied in other fields of structural biology, such as cryo-

electron microscopy [95–97], small angle X-ray scattering [98] or, to some extent, neutron diffraction [99,100]. The interfacial architecture probed in an NR experiment is typically more complex than desirable for MD simulations, which poses a particular challenge. Another structural difficulty arises from the fact that NR data contains structural information of an ensemble average. Therefore, any biased MD simulation needs to be steered by either a time average of a single copy or by an ensemble average of multiple copies of the simulated system. Both approaches are computationally challenging for most systems of interest. Coarse-grained MD simulations or Monte-Carlo simulations might be required to overcome such limitations.

### 3.6. Triggered conformational changes

The most extensively studied conformational change in a membrane-associated protein with NR to date is the transition of HIV-1 Nef from its closed form to an open form [25,26]. Using a Langmuir monolayer as a model system whose lateral pressure can be precisely controlled, it was demonstrated that it is specifically the insertion of the Nef myristate into the lipid bilayer which triggers the conformational change of the protein. In the course of this reorganization, a compact core domain of Nef is displaced by about 70 Å from the lipid membrane, as shown schematically in Fig. 6. Environmental variables, such as the density of charged lipids in the membrane or protein concentration in the adjacent buffer, were not sufficient by themselves to trigger similar changes in protein conformation. Again, molecular modeling techniques [101] and MD simulations were essential to determine the ensemble of conformations that reproduce the NR data.

## 4. Conclusions

Neutron reflection techniques have come a long way from assessing phospholipid chain order and headgroup conformation in floating Langmuir monolayers [102] to providing detailed molecular models of protein complexes on fluid bilayer lipid membranes [21,23]. While the intrinsic optical resolution in NR is limited by an accessible momentum transfer range that is largely determined by the incoherent background and therefore cannot be significantly enhanced, we showed here that other improvements have indeed driven the field in recent years. Most importantly, a rigorous and self-consistent modeling strategy permits to utilize internal protein structures, resolved by crystallography or NMR, to obtain structures of protein/membrane complexes. While this assumes that the crystal structure is conserved in the membrane-

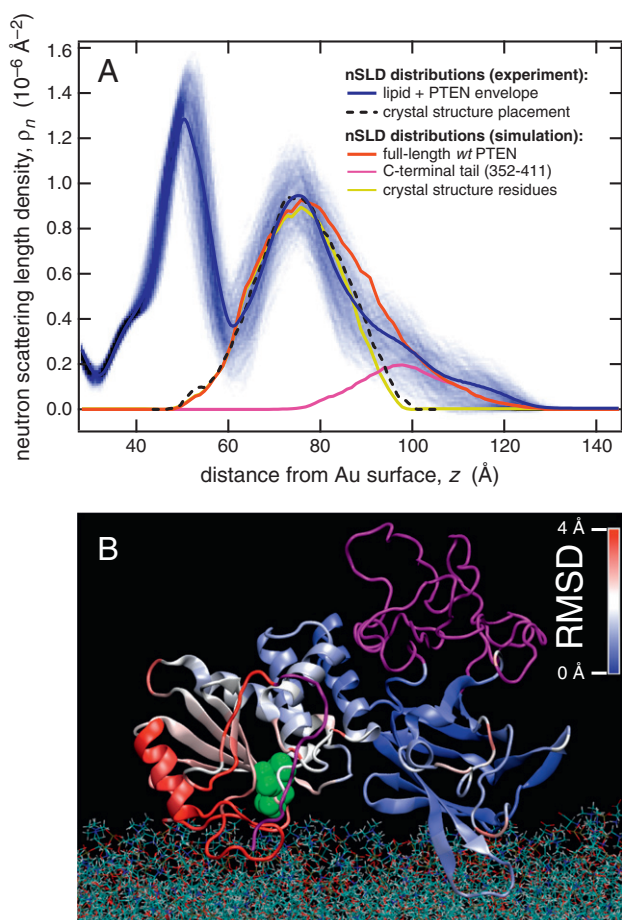


**Fig. 5.** (A) Comparison of nSLD profiles derived from experimental data [21] and computed from time averaged MD trajectories [23]. The horizontal axis has its origin at the gold surface of the experimental system. The blue line shows the most probable nSLD distribution given the experimental data, and the shaded blue band indicates the 68% confidence limits of the envelope. The dashed line shows the tentative placement of the crystal structure of a truncated PTEN [22] optimized to retrace the experimental nSLD profile around its peak near  $z = 75$  Å, which has been attributed to the membrane-bound protein [21]. Based on the placement of the headgroups in the simulation results, the remaining traces show CVO distributions of other portions of the protein, as indicated: full-length PTEN protein, PTEN's two core domains, *i.e.*, its C2 and phosphatase domains and the unstructured C-terminal tail. (B) Snapshot from an MD simulation that reproduces the time-averaged NR envelope of the protein. The unstructured segments are shown in purple. Two Cys residues, shown in green, mark the catalytic site. The remainder of the protein, *i.e.*, the PTEN core domains, is color encoded according to the deviations of  $C\alpha$  positions from those observed in the crystal structure (scale bar). While the membrane-bound models deviate somewhat from the crystal structure, major portions of the C2 domain (right) and, less so, of the phosphatase domain (left) are rigid. This is also true for the interface between the two core domains. In the membrane-bound state, the single major adjustment of the structure concerns the region around the  $\alpha 1$  helix, to the far left of the model that leads to a flattening of the overall protein structure against the membrane.

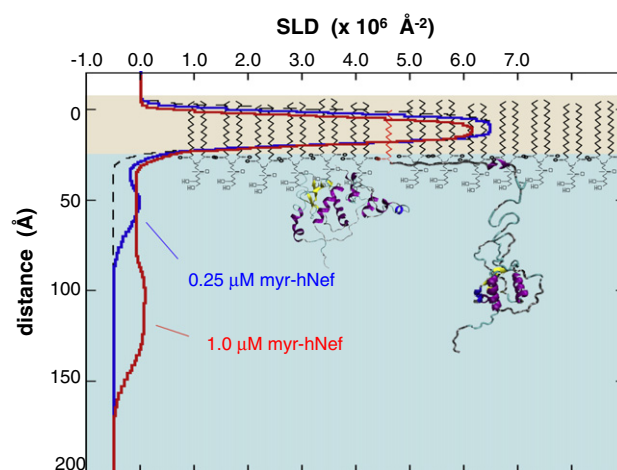


**Fig. 6.** NR results for the myristoylated HIV-1 Nef adsorbed to a DPPG monolayer on Tris-buffered  $\text{H}_2\text{O}$  subphase (black dashed) and with myristoylated HIV-1 Nef adsorbed from solutions at 0.25  $\mu\text{M}$ /L (blue) and at 1.0  $\mu\text{M}$ /L (red). The molecular models of DPPG and of Nef were scaled to coincide approximately with the corresponding features in the SLD profiles. Figure reproduced with permission from [25].

bound protein, MD simulations provide a sanity check to determine to which extent this is appropriate. For example, for the PTEN tumor suppressor, it was thus shown that the protein structures both in solution and on the membrane differ slightly from the crystal structure. However, in that particular example, these differences were small and, in any case, below the optical resolution. Model-free data refinement is both a valuable analytical tool on its own and a complement for situations where internal protein structures are only partially known. Another important development is the objective assessment of uncertainties in model parameters and, more generally, confidence bands on the determined best-fit nSLD on CVO profiles. With these tools now at hand, structures of protein/membrane complexes on in-plane fluid bilayers can be determined with unprecedented precision.

## Acknowledgments

This work was supported by the DOE (70NANB13H009) and NIH (1R01 GM101647) and performed in parts at the NIST Center for Neutron Research and the NIST Center for Nanoscale Science and Technology.

## References

- [1] B. Alberts, D. Bray, J. Lewis, M. Raff, J.D. Watson, *Molecular Biology of the Cell*, Garland, New York, 1983.
- [2] R. Shaw, L.C. Cantley, Ras, PI(3)K and mTOR signalling controls tumour cell growth, *Nature* 441 (2006) 424–430.
- [3] M.P. Wymann, R. Schneider, Lipid signalling in disease, *Nat. Rev. Mol. Cell Biol.* 9 (2008) 162–176.
- [4] B. Vanhaesebroeck, L. Stephens, P. Hawkins, PI3K signalling: the path to discovery and understanding, *Nat. Rev. Mol. Cell Biol.* 13 (2012) 195–203.
- [5] A. Hodgkin, A. Huxley, A quantitative description of membrane current and its application to conduction and excitation in nerve, *J. Physiol.* 117 (1952) 500–544.
- [6] L. De Haan, T.R. Hirst, Cholera toxin: a paradigm for multi-functional engagement of cellular mechanisms, *Mol. Membr. Biol.* 21 (2004) 77–92.
- [7] J. Deisenhofer, H. Michel, Nobel lecture. The photosynthetic reaction centre from the purple bacterium *Rhodospseudomonas viridis*, *EMBO J.* 8 (1989) 2149–2170.
- [8] J. Deisenhofer, H. Michel, The photosynthetic reaction center from the purple bacterium *Rhodospseudomonas viridis*, *Science* 245 (1989) 1463–1473.
- [9] S.H. White, Membrane proteins of known structure, <http://blanco.biomol.uci.edu/mpstruc/> (accessed: February, 2014).
- [10] N. Grigorieff, T.A. Ceska, K.H. Downing, J.M. Baldwin, R. Henderson, Electron-crystallographic refinement of the structure of Bacteriorhodopsin, *J. Mol. Biol.* 259 (1996) 393–421.
- [11] J.L.S. Milne, M.J. Borgnia, A. Bartesaghi, E.E.H. Tran, L.A. Earl, et al., Cryo-electron microscopy—a primer for the non-microscopist, *FEBS J.* 280 (2013) 28–45.
- [12] E. Pebay-Peyroula, G. Rummel, J.P. Rosenbusch, E.M. Landau, X-ray structure of bacteriorhodopsin at 2.5 Å resolution from microcrystals grown in lipidic cubic phases, *Science* 277 (1997) 1676–1681.
- [13] S.J. Opella, Structure determination of membrane proteins by nuclear magnetic resonance spectroscopy, *Annu. Rev. Anal. Chem.* 6 (2013) 305–328.
- [14] F. Hagn, M. Etzkorn, T. Raschle, G. Wagner, Optimized phospholipid bilayer nanodiscs facilitate high-resolution structure determination of membrane proteins, *J. Am. Chem. Soc.* 135 (2013) 1919–1925.
- [15] S. Shenoy, R. Moldovan, J. Fitzpatrick, D.J. Vanderah, M. Deserno, M. Lösche, In-plane homogeneity and lipid dynamics in tethered bilayer lipid membranes (tBLMs), *Soft Matter* 6 (2010) 1263–1274.
- [16] D.J. McGillivray, G. Valincius, F. Heinrich, J.W.F. Robertson, D.J. Vanderah, et al., Structure of functional *Staphylococcus aureus*  $\alpha$ -hemolysin channels in tethered bilayer lipid membranes, *Biophys. J.* 96 (2009) 1547–1553.
- [17] C. Chen, S. Malkova, S. Pingali, F. Long, S. Garde, et al., Configuration of PKC $\alpha$ -C2 domain bound to mixed SOPC/SOPS lipid monolayers, *Biophys. J.* 97 (2009) 2794–2802.
- [18] S. Málková, R.V. Stahelin, S.V. Pingali, W. Cho, M.L. Schlossman, Orientation and penetration depth of monolayer-bound p40phox-PX, *Biochemistry* 45 (2006) 13566–13575.
- [19] F. Heinrich, H. Nanda, H.Z. Goh, C. Bachert, M. Lösche, A.D. Linstedt, Myristoylation restricts orientation of the GRASP domain on membranes and promotes membrane tethering, *J. Biol. Chem.* 289 (14) (2014) 9683–9691.
- [20] H. Nanda, S.A.K. Datta, F. Heinrich, M. Lösche, A. Rein, et al., Electrostatic interactions and binding orientation of HIV-1 matrix, studied by neutron reflectivity, *Biophys. J.* 99 (2010) 2516–2524.
- [21] S. Shenoy, P. Shekhar, F. Heinrich, M.-C. Daou, A. Gericke, et al., Membrane association of the PTEN tumor suppressor: molecular details of the protein–membrane complex from SPR binding studies and neutron reflection, *PLoS ONE* 7 (2012) e32591.
- [22] J.O. Lee, H. Yang, M.M. Georgescu, A. Di Cristofano, T. Maehama, et al., Crystal structure of the PTEN tumor suppressor: implications for its phosphoinositide phosphatase activity and membrane association, *Cell* 99 (1999) 323–334.
- [23] S. Shenoy, H. Nanda, M. Lösche, Membrane association of the PTEN tumor suppressor: electrostatic interaction with phosphatidylserine-containing bilayers and regulatory role of the C-terminal tail, *J. Struct. Biol.* 180 (2012) 394–408.
- [24] S.A.K. Datta, F. Heinrich, S. Raghunandan, S. Krueger, J.E. Curtis, et al., HIV-1 Gag extension: conformational changes require simultaneous interaction with membrane and nucleic acid, *J. Mol. Biol.* 406 (2011) 205–214.
- [25] M.S. Kent, J.K. Murton, D.Y. Sasaki, S. Satija, B. Akgun, et al., Neutron reflectometry study of the conformation of HIV Nef bound to lipid membranes, *Biophys. J.* 99 (2010) 1940–1948.
- [26] B. Akgun, S. Satija, H. Nanda, G.F. Pirrone, X. Shi, et al., Conformational transition of membrane-associated terminally acylated HIV-1 Nef, *Structure* 21 (2013) 1822–1833.
- [27] C.F. Majkrzak, E. Carpenter, F. Heinrich, N.F. Berk, When beauty is only skin deep; optimizing the sensitivity of specular neutron reflectivity for probing structure beneath the surface of thin films, *J. Appl. Phys.* 110 (2011) 102212.
- [28] G.J. Hardy, R. Nayak, S. Munir Alam, J.G. Shapter, F. Heinrich, S. Zauscher, Biomimetic supported lipid bilayers with high cholesterol content, *J. Mater. Chem.* 22 (2012) 19506–19513.
- [29] N.A. Anderson, L.J. Richter, J.C. Stephenson, K.A. Briggman, Determination of lipid phase transition temperatures in hybrid bilayer membranes, *Langmuir* 22 (2006) 8333–8336.
- [30] N.A. Anderson, L.J. Richter, J.C. Stephenson, K.A. Briggman, Characterization and control of lipid layer fluidity in hybrid bilayer membranes, *J. Am. Chem. Soc.* 129 (2007) 2094–2100.
- [31] S. Krueger, C.W. Meuse, C.F. Majkrzak, J.A. Dura, N.F. Berk, et al., Investigation of hybrid bilayer membranes with neutron reflectometry: probing the interactions of melittin, *Langmuir* 17 (2001) 511–521.
- [32] C.W. Meuse, S. Krueger, C.F. Majkrzak, J.A. Dura, J. Fu, et al., Hybrid bilayer membranes in air and water: infrared spectroscopy and neutron reflectivity studies, *Biophys. J.* 74 (1998) 1388–1398.
- [33] C.F. Majkrzak, N.F. Berk, S. Krueger, J.A. Dura, M. Tarek, et al., First-principles determination of hybrid bilayer membrane structure by phase-sensitive neutron reflectometry, *Biophys. J.* 79 (2000) 3330–3340.
- [34] I. Köper, Insulating tethered bilayer lipid membranes to study membrane proteins, *Mol. Biosyst.* 3 (2007) 651–657.
- [35] C. Rossi, J. Chopineau, Biomimetic tethered lipid membranes designed for membrane–protein interaction studies, *Eur. Biophys. J. Biophys. Lett.* 36 (2007) 955–965.
- [36] M. Tanaka, E. Sackmann, Polymer-supported membranes as models of the cell surface, *Nature* 437 (2005) 656–663.
- [37] C.A. Naumann, O. Prucker, T. Lehmann, J. Rühle, W. Knoll, C.W. Frank, The polymer-supported phospholipid bilayer: tethering as a new approach to substrate-membrane stabilization, *Biomacromolecules* 3 (2002) 27–35.
- [38] M.L. Wagner, L.K. Tamm, Tethered polymer-supported planar lipid bilayers for reconstitution of integral membrane proteins: silane-polyethyleneglycol-lipid as a cushion and covalent linker, *Biophys. J.* 79 (2000) 1400–1414.
- [39] J. Majewski, J.Y. Wong, C.K. Park, M. Seitz, J.N. Israelachvili, G.S. Smith, Structural studies of polymer-cushioned lipid bilayers, *Biophys. J.* 75 (1998) 2363–2367.
- [40] G. Fragneto, T. Charitat, F. Graner, K. Mecke, L. Perino-Galice, E. Bellet-Amalric, A floating lipid bilayer, *Europhys. Lett.* 53 (2001) 100–106.
- [41] A.V. Hughes, J.R. Howse, A. Dabkowska, R. Jones, M.J. Lawrence, S.J. Roser, Floating lipid bilayers deposited on chemically grafted phosphatidylcholine surfaces, *Langmuir* 24 (2008) 1989–1999.
- [42] H.P. Wacklin, Neutron reflection from supported lipid membranes, *Curr. Opin. Colloid Interface Sci.* 15 (2010) 445–454.
- [43] W. Knoll, R. Naumann, M. Friedrich, J.W.F. Robertson, M. Lösche, et al., Solid supported functional lipid membranes based on monomolecular protein sheet crystals: new concepts for the biomimetic functionalization of solid surfaces, *Biointerphases* 3 (2008) FA125–FA135.
- [44] E.T. Castellana, P.S. Cremer, Solid supported lipid bilayers: from biophysical studies to sensor design, *Surf. Sci. Rep.* 61 (2006) 429–444.
- [45] A. Brun, T.A. Darwish, M. James, Studies of biomimetic cellular membranes using neutron reflection, *J. Chem. Biol. Interface* 1 (2013) 3–24.
- [46] M. Weygand, B. Wetzler, D. Pum, U.B. Sleytr, N. Cuvillier, et al., Bacterial S-layer protein coupling to lipids: X-ray reflectivity and grazing incidence diffraction studies, *Biophys. J.* 76 (1999) 458–468.
- [47] D.J. McGillivray, G. Valincius, D.J. Vanderah, W. Febo-Ayala, J.T. Woodward, et al., Molecular-scale structural and functional characterization of sparsely tethered bilayer lipid membranes, *Biointerphases* 2 (2007) 21–33.
- [48] F. Heinrich, T. Ng, D.J. Vanderah, P. Shekhar, M. Mihailescu, et al., A new lipid anchor for sparsely tethered bilayer lipid membranes, *Langmuir* 25 (2009) 4219–4229.
- [49] R. Budvytyte, G. Valincius, G. Niaura, V. Voiciuk, M. Mickevicius, et al., Structure and properties of tethered bilayer lipid membranes with unsaturated anchor molecules, *Langmuir* 29 (2013) 8645–8656.
- [50] G. Valincius, T. Meskauskas, F. Ivanauskas, Electrochemical impedance spectroscopy of tethered bilayer membranes, *Langmuir* 28 (2012) 977–990.
- [51] G. Valincius, F. Heinrich, R. Budvytyte, D.J. Vanderah, D.J. McGillivray, et al., Soluble amyloid  $\beta$ -oligomers affect dielectric membrane properties by bilayer insertion and domain formation: implications for cell toxicity, *Biophys. J.* 95 (2008) 4845–4861.
- [52] R. Budvytyte, M. Mickevicius, D.J. Vanderah, F. Heinrich, G. Valincius, Modification of tethered bilayers by phospholipid exchange with vesicles, *Langmuir* 29 (2013) 4320–4327.
- [53] K.J. Kwak, G. Valincius, W.-C. Liao, X. Hu, X. Wen, et al., Formation and finite element analysis of tethered bilayer lipid structures, *Langmuir* 26 (2010) 18199–18208.
- [54] C.M. Majkrzak, N.F. Berk, S. Krueger, U.A. Perez-Salas, Structural investigations of membranes of interest in biology by neutron reflectometry, in: J. Fitter, T.

- Gutberlet, J. Katsaras (Eds.), *Neutron Scattering in Biology*, Springer, New York, 2006, pp. 225–264.
- [55] J.H. Lakey, Neutrons for biologists: a beginner's guide, or why you should consider using neutrons, *J. R. Soc. Interface* 6 (2009) S567–S573.
- [56] J.A. Dura, D. Pierce, C.F. Majkrzak, N. Maliszewskij, D.J. McGillivray, et al., AND/R: a neutron diffractometer/reflector for investigation of thin films and multilayers for the life sciences, *Rev. Sci. Instrum.* 77 (2006) 074301.
- [57] B.J. Kirby, P.A. Kienzle, B.B. Maranville, N.F. Berk, J. Krycka, et al., Phase-sensitive specular neutron reflectometry for imaging the nanometer scale composition depth profile of thin-film materials, *Curr. Opin. Colloid Interface Sci.* 17 (2012) 44–53.
- [58] S.A. Holt, A.P. Le Brun, C.F. Majkrzak, D.J. McGillivray, F. Heinrich, et al., An ion channel containing model membrane: structural determination by magnetic contrast neutron reflectometry, *Soft Matter* 5 (2009) 2576–2586.
- [59] A. Le Brun, S.A. Holt, D.S.H. Shah, C.F. Majkrzak, J.H. Lakey, The structural orientation of antibody layers bound to engineered biosensor surfaces, *Biomaterials* 32 (2011) 3303–3311.
- [60] J. Ankner, C.F. Majkrzak, Subsurface profile refinement for neutron specular reflectivity, *Proc. SPIE* 1738 (1992) 260–269.
- [61] M.C. Wiener, S.H. White, Structure of a fluid dioleoylphosphatidylcholine bilayer determined by joint refinement of X-ray and neutron diffraction data. III. Complete structure, *Biophys. J.* 61 (1992) 434–447.
- [62] M. Schälke, P. Krüger, M. Weygand, M. Lösche, Submolecular organization of DMPA in surface monolayers: beyond the two-layer model, *Biochim. Biophys. Acta* 1464 (2000) 113–126.
- [63] P. Shekhar, H. Nanda, M. Lösche, F. Heinrich, Continuous distribution model for the investigation of complex molecular architectures near interfaces with scattering techniques, *J. Appl. Phys.* 110 (2011) 102216.
- [64] H.-H. Shen, R.K. Thomas, C.-Y. Chen, R.C. Darton, S.C. Baker, J. Penfold, Aggregation of the naturally occurring lipopeptide, surfactin, at interfaces and in solution: an unusual type of surfactant? *Langmuir* 25 (2009) 4211–4218.
- [65] N. Kučerka, J.F. Nagle, J.N. Sachs, S.E. Feller, J. Pencer, et al., Lipid bilayer structure determined by the simultaneous analysis of neutron and X-ray scattering data, *Biophys. J.* 95 (2008) 2356–2367.
- [66] J.F. Nagle, S. Tristram-Nagle, Structure of lipid bilayers, *Biochim. Biophys. Acta* 1469 (2000) 159–195.
- [67] N. Kučerka, J. Katsaras, J.F. Nagle, Comparing membrane simulations to scattering experiments: introducing the SIMtoEXP software, *J. Membr. Biol.* 235 (2010) 43–50.
- [68] V.F. Sears, Neutron scattering lengths and cross sections, *Neutron News* 3 (1992) 26–37.
- [69] M. Connolly, Solvent-accessible surfaces of proteins and nucleic acids, *Science* 221 (1983) 709–713.
- [70] M.L. Connolly, Analytical molecular-surface calculation, *J. Appl. Crystallogr.* 16 (1983) 548–558.
- [71] S.J. Perkins, Protein volumes and hydration effects. The calculations of partial specific volumes, neutron scattering matchpoints and 280-nm absorption coefficients for proteins and glycoproteins from amino acid sequences, *Eur. J. Biochem.* 157 (1986) 169–180.
- [72] F. Lekien, J. Marsden, Tricubic interpolation in three dimensions, *Int. J. Numer. Methods Eng.* 63 (2005) 455–471.
- [73] C.F. Laub, T.L. Kuhl, Fitting a free-form scattering length density profile to reflectivity data using temperature-proportional quenching, *J. Chem. Phys.* 125 (2006) 244702.
- [74] A. Van der Lee, F. Salah, B. Harzallah, A comparison of modern data analysis methods for X-ray and neutron specular reflectivity data, *J. Appl. Crystallogr.* 40 (2007) 820–833.
- [75] S.M. Danauskas, D. Li, M. Meron, B. Lin, K.Y.C. Lee, Stochastic fitting of specular X-ray reflectivity data using StochFit, *J. Appl. Crystallogr.* 41 (2008) 1187–1193.
- [76] N.F. Berk, C.F. Majkrzak, Using parametric B splines to fit specular reflectivities, *Phys. Rev. B* 51 (1995) 11296–11309.
- [77] J. Skov Pedersen, Model-independent determination of the surface scattering-length-density profile from specular reflectivity data, *J. Appl. Crystallogr.* 25 (1992) 129–145.
- [78] J. Skov Pedersen, I.W. Hamley, Analysis of neutron and X-ray reflectivity data. II. Constrained least-square methods, *J. Appl. Crystallogr.* 27 (1994) 36–49.
- [79] B.W. Koenig, S. Krueger, W.J. Orts, C.F. Majkrzak, N.F. Berk, et al., Neutron reflectivity and atomic force microscopy studies of a lipid bilayer in water adsorbed to the surface of a silicon single crystal, *Langmuir* 12 (1996) 1343–1350.
- [80] E. Catmull, R. Rom, A class of local interpolating splines, in: R.E. Barnhill, R.F. Reisenfeld (Eds.), *Computer-Aided Geometric Design*, Academic Press, New York, 1974, pp. 317–326.
- [81] F. Fritsch, R. Carlson, Monotone piecewise cubic interpolation, *SIAM J. Numer. Anal.* 17 (1980) 238–246.
- [82] E. Politsch, StringFit: a new structurally oriented X-ray and neutron reflectivity evaluation technique, *J. Appl. Crystallogr.* 34 (2001) 239–251.
- [83] E. Politsch, G. Cevc, Determination of the molecular arrangement from neutron or X-ray reflectivity, *Physica B* 276 (2000) 390–391.
- [84] E. Politsch, G. Cevc, A. Wurlitzer, M. Lösche, Conformation of polymer brushes at aqueous surfaces determined with X-ray and neutron reflectometry. I. Novel data evaluation procedure for polymers at interfaces, *Macromolecules* 34 (2001) 1328–1333.
- [85] A. Wurlitzer, E. Politsch, S. Hübner, P. Krüger, M. Weygand, et al., Conformation of polymer brushes at aqueous surfaces determined with X-ray and neutron reflectometry. II. High density phase transition of lipopolyoxazolines, *Macromolecules* 34 (2001) 1334–1342.
- [86] E. Politsch, Structure-related simultaneous X-ray and neutron reflectivity analysis method for Langmuir films, *Langmuir* 19 (2003) 1221–1226.
- [87] M. Lösche, M. Piepenstock, A. Diederich, T. Grünwald, K. Kjaer, D. Vaknin, Influence of surface chemistry on the structural organization of monomolecular protein layers adsorbed to functionalized aqueous interfaces, *Biophys. J.* 65 (1993) 2160–2177.
- [88] S.M. Bezrukov, I. Vodyanov, R.A. Brutyan, J.J. Kasianowicz, Dynamics and free energy of polymers partitioning into a nanoscale pore, *Macromolecules* 29 (1996) 8517–8522.
- [89] L. Song, M.R. Hobaugh, C. Shustak, S. Cheley, H. Bayley, J.E. Gouaux, Structure of staphylococcal  $\alpha$ -hemolysin, a heptameric transmembrane pore, *Science* 274 (1996) 1859–1865.
- [90] J.S. Saad, J. Miller, J. Tai, A. Kim, R.H. Ghanam, M.F. Summers, Structural basis for targeting HIV-1 Gag proteins to the plasma membrane for virus assembly, *Proc. Natl. Acad. Sci. U. S. A.* 103 (2006) 11364–11369.
- [91] C.M. Pfefferkorn, F. Heinrich, A.J. Sodd, A.S. Maltsev, R.W. Pastor, J.C. Lee, Depth of  $\alpha$ -synuclein in a bilayer determined by fluorescence, neutron reflectometry, and computation, *Biophys. J.* 102 (2012) 613–621.
- [92] M.C. Wiener, G.I. King, S.H. White, Structure of a fluid dioleoylphosphatidylcholine bilayer determined by joint refinement of X-ray and neutron diffraction data. I. Scaling of neutron data and the distribution of double bonds and water, *Biophys. J.* 60 (1991) 568–576.
- [93] M.C. Wiener, S.H. White, Structure of a fluid dioleoylphosphatidylcholine bilayer determined by joint refinement of X-ray and neutron diffraction data. II. Distribution and packing of terminal methyl groups, *Biophys. J.* 61 (1992) 428–433.
- [94] N. Kučerka, S. Tristram-Nagle, J.F. Nagle, Structure of fully hydrated fluid phase lipid bilayers with monounsaturated chains, *J. Membr. Biol.* 208 (2005) 193–202.
- [95] K.-Y. Chan, L.G. Trabuco, E. Schreiner, K. Schulten, Cryo-electron microscopy modeling by the molecular dynamics flexible fitting method, *Biopolymers* 97 (2012) 678–686.
- [96] L.G. Trabuco, E. Villa, E. Schreiner, C.B. Harrison, K. Schulten, Molecular dynamics flexible fitting: a practical guide to combine cryo-electron microscopy and X-ray crystallography, *Methods* 49 (2009) 174–180.
- [97] W. Zheng, Accurate flexible fitting of high-resolution protein structures into cryo-electron microscopy maps using coarse-grained pseudo-energy minimization, *Biophys. J.* 100 (2011) 478–488.
- [98] W. Zheng, M. Tekpinar, Accurate flexible fitting of high-resolution protein structures to small-angle X-ray scattering data using a coarse-grained model with implicit hydration shell, *Biophys. J.* 101 (2011) 2981–2991.
- [99] R. Benz, F. Castro-Román, D.J. Tobias, S.H. White, Experimental validation of molecular dynamics simulations of lipid bilayers: a new approach, *Biophys. J.* 88 (2005) 805–817.
- [100] R.W. Benz, H. Nanda, F. Castro-Roman, S.H. White, D.J. Tobias, Diffraction-based density restraints for membrane and membrane-peptide molecular dynamics simulations, *Biophys. J.* 91 (2006) 3617–3629.
- [101] J.E. Curtis, S. Raghunathan, H. Nanda, S. Krueger, SASSIE: a program to study intrinsically disordered biological molecules and macromolecular ensembles using experimental scattering constraints, *Comput. Phys. Commun.* 183 (2012) 382–389.
- [102] D. Vaknin, K. Kjaer, J. Als-Nielsen, M. Lösche, Structural properties of phosphatidylcholine in a monolayer at the air/water interface. Neutron reflection study and re-examination of X-ray reflection experiments, *Biophys. J.* 59 (1991) 1325–1332.